Estimation of aerosol radiative effects on the terrestrial gross primary productivity in China

Zhaoyang Zhang[a*], Muyuan Gao[a], Qiaozhen Liu[a], Yunhui Tan[a], Enguang Li[a], Quan Wang[b*]

a. College of Geography and Environmental Sciences, Zhejiang Normal University, Zhejiang Province, China
b. Faculty of Agriculture, Shizuoka University, Shizuoka, Japan

*Corresponding author: Zhaoyang Zhang (zhzhyang@outlook.com), Quan Wang (wang.quan@shizuoka.ac.jp)

Key Points:

- MODIS Atmosphere and Land products combined with the process-based model were used to accurately evaluate the aerosol effects to GPP.
- The aerosol radiative effects on GPP not only varied with vegetation type but also varied with spectral regions.
- Cloud restrains the effects of aerosols on growth of plants.

Abstract

China experienced heavy aerosol pollution in recent years. The aerosol pollution might change surface solar radiation and impact the land carbon cycle in China. Therefore, we combined the MODIS Atmosphere and Land products with process-based model to evaluate the sensitivity of GPP to AOD in different spectral bands under all-sky and cloudless conditions and the effects of current aerosol loadings on GPP at site level. Our results indicated that the radiative effects of aerosols on GPP varied with the vegetation type, which is consistent with other studies. We also found that the radiative effects of aerosols on GPP varied with the spectral bands. Cloud restrains the effects of aerosols on growth of plants. Current aerosol loadings fertilized the growth in two forest growth and slightly impede the growth of grass. The results in this paper could be help to fully understand the influences of aerosol on land carbon cycle.

Plain Language Summary

Due to the heavy aerosol pollution in China, understanding and quantifying the aerosol direct effect on plants GPP is very important in this region. To achieve this goal, MODIS Land and Atmosphere products combined with the process-based model were used. We firstly found the aerosol radiative effects on GPP not only varied with the vegetation types but also varied with the spectral regions, such as PAR and NIR. We also found that the cloud will weak the aerosol effects on GPP. The result cloud help for understanding the aerosol effects on land carbon uptake.

1. Introduction

Atmospheric aerosols contain varieties of shapes, compositions, sizes and optical properties [*Hinds,* 1999]. Until now, aerosol still is one of the largest uncertainties in climate studies [*Field et al.*, 2014]. Aerosols can affect the climate changes through direct [*Yu,* 2004]and indirect effects [*Huang et al.,* 2006; *Zamora et al.*, 2017]. The direct effect is that aerosols can affect the atmospheric radiative balance through absorbing and scattering the solar radiation [*Chou et al.*, 2006; *Qian et al.*, 2007]. Solar radiation is an essential factor for plants photosynthesis. The disturbance of solar radiation can affect plant physiological processes in two ways. First, the increasing aerosol loadings can reduce total solar radiation [*Eck et al.*, 2013]. Second, the increasing aerosol loadings could also increase the diffuse radiation [*Ceamanos et al.*, 2014]. Increased fraction of diffuse radiation could enhance photosynthesis to some extent [*Yamaguchi and Izuta*, 2017]. This was called as the diffuse radiation fertilization effect [*Mercado et al.*, 2009].

Previous studies of aerosol effects on plant productivity have been conducted in many regions [*Cohan et al.*, 2002; *Ezhova et al.*, 2018; *O'Sullivan et al.*, 2016; *Rap et al.*, 2018; *X. Yue and Unger*, 2017]. *Cohan et al.* [2002] found that soybean net primary productivity (NPP) peaks under moderately thick aerosol loadings using multilayer canopy model. *Niyogi et al.* [2004] indicated that CO_2 sink increased with aerosol loadings for forest and crop land, and decreased for grassland through analyzing multi-site observations. *Misson et al.* [2005] showed that the increase in diffuse radiation due to aerosol can increase by 8% of CO_2 net uptake. *Cirino et al.* [2014] found that the aerosol effect accounted an approximate 20% increase in net ecosystem exchange (NEE) in Amazon. *Strada et al.* [2015] found that high aerosol optical depth (AOD) enhanced plant productivity by 13% in deciduous forests and had no significant effects on cropland and grassland using the satellite and surface measurements. *Ezhova et al.* [2018] also observed larger increase in GPP for coniferous and mixed forest. *Xu Yue and Unger* [2018] also found that aerosol increased GPP by 0.05 ± 0.30 Pg C yr^{-1}.

China suffered heavy polluted conditions in recent years [*Zhang et al.*, 2015; *Zhang et al.*, 2019b]. The comprehensive understanding of aerosol climatology and their effects over China is very import for evaluating the global role of aerosol in environmental, climatic and terrestrial problems [*Liu et al.*, 2009; *Tang et al.*, 2014; *X X Tie and Cao*, 2009; *Wu et al.*, 2014]. Most of the research focused on investigating the aerosol effect on environmental and climatic problems. Only few studies investigated the effects on ecosystem in China [*X Tie et al.*, 2016]. *Chameides et al.* [1999] estimated the influence of aerosol pollution on crop yields by using coupled regional climate and air quality model. *X Tie et al.* [2016] investigated the effect of regional haze pollution on rice and wheat over China using satellite measurements and empirical model. *X. Yue and Unger* [2017] also access the radiative effects of aerosol pollution using combined vegetation and radiation model.

However, most of these studies used the aerosol from reanalysis data or simulated by model. Although they can reflect the general spatial and temporal variations of aerosols, the AOD was largely underestimated [*Che et al.*, 2019]. What is more, these studies are mainly investigate the aerosol radiative effects on plants growth at 300-700 nm or 300-4000nm wavelength. Therefore, there are still large uncertainties in evaluating the influence of aerosols on land carbon uptake and the radiative effects at different spectral wavelengths in GPP is still unclear.

The objective in this study is to evaluate the aerosol direct effects on terrestrial gross primary productivity at site level over China, especially for different spectral wavelengths. We used Santa Barbara DISORT Atmospheric Radiative Transfer (SBDART) model and Breathing Earth System Simulator (BESS) to access the current aerosol pollution direct effects on GPP at 10 FLUXNET sites in China. Firstly, we perform sensitivity experiments to investigate the sensitivity of GPP to AOD under all-sky and cloudless conditions for each site. Then, we simulate the GPP with and without aerosol. In addition to photosynthetically active radiation (PAR), we also consider the effect of near-infrared radiation (NIR). Section 2 describes the satellite Atmosphere and Land products, radiative transfer model, and process-based model used in this paper. Section 3 shows the results of sensitivity experiments. The effects

of PAR and NIR induced by aerosol are shown in Section 4. Section 5 summarizes and discusses the main results.

2. Data and methods

2.1 FLUXNET data

FLUXNET was established to monitor the temperature, humidity, wind speed, rainfall, and atmospheric carbon dioxide using the ground-based instruments and the data from FLUXNET can be used as a reference to validate the satellite and model data. We used 10 FLUXNET stations to examine the GPP products from BESS model. Table 1 shows the specific information of these FLUXNET sites. Here, the GPP_NT_VUT_REF in FLUXNET2015 dataset was used.

Table 1. The locations and surface type of FLUXNET in China.

Station name	Surface type	Latitude	Longitude
CN-Cha	MF	42.4025	128.0958
CN-Cng	GRA	44.5934	123.5092
CN-Dan	GRA	30.4978	91.0664
CN-Din	EBF	23.1733	112.5361
CN-Du2	GRA	42.0467	116.2836
CN-Du3	GRA	42.0551	116.2809
CN-Ha2	WET	37.6086	101.3269
CN-HaM	GRA	37.37	101.18
CN-Qia	ENF	26.7414	115.0581
CN-Sw2	GRA	41.7902	111.8971

2.2 MODIS products

In this paper, MODIS data were used to calculate the PAR (300-700 nm) and NIR (700-4000 nm). We used MODIS Atmosphere and Land products, including solar zenith angle (MOD07), cloud optical thickness (MOD06), white-sky albedo and black-sky albedo for visible and near infrared albedo (MCD43C3), aerosol optical depth (MCD19A2), total ozone burden (MOD07), and total column precipitable water

vapor (MOD07). The station values were extracted from the nearest pixels around the FLUXNET station in the MODIS products. Because the high accuracy of Multi-Angle Implementation of Atmospheric Correction (MAIAC) AOD [*Martins et al.*, 2017; *Zhang et al.*, 2019a], the data were selected to accurately simulate the radiative effects induced by the aerosols in this paper.

2.3 SBDART model

Santa Barbara DISORT Atmospheric Radiative Transfer (SBDART) model was developed by Institute for Computational Earth System Science, University of California in 1998. The model was designed for processing and analyzing radiative transfer problems of satellite remote sensing and atmospheric energy balance. The model can be used for calculating the radiation reached at the surface under both all-sky and cloudless days [*Ricchiazzi et al.*, 1998]. This model considers all the important absorption and scattering processes which affects UV, visible and infrared radiation. SBDART can calculate the radiance reached at the surface from 0.2μm to 100μm with an interval of 5nm-200nm. SBDART has been used for many researches and good performance was shown [*Frouin and Murakami*, 2007; *Nagorski et al.*, 2019; *Wong et al.*, 2008]. The aerosol type was set as rural aerosol. In this study, SBDART model was used to simulate the radiance at ground surface.

2.4 BESS model

In this paper, process-based model was used because it is able to provide response to environment changes, such as global warming and elevated carbon dioxide. The Breathing Earth System Simulator (BESS) is a simplified process-based model, which can simulate the canopy carbon and water fluxes, and quantified the PAR and NIR effects for sunlit and shade leaves. The model was developed by *Ryu et al.* [2018] and integrated with remote sensing data. The model can take full advantages of MODIS products [*Jiang and Ryu*, 2016]. *Ryu et al.* [2011] and *Jiang and Ryu* [2016] evaluated the performance of BESS model using FLUXNET observations and the results indicated that the model simulations were comparable with FLUXNET observations and MPI-BGC products. The BESS model code can be freely obtained from the environmental ecology lab in Seoul national university

148 (http://environment.snu.ac.kr/bess_flux/). Some input data for FLUXNET sites were
149 also included in the package. To investigate the aerosol radiative effects on GPP, we
150 did four experiments (Table 2).

151 Table 2. Experiments design for this study.

Experiments	Description
E1	GPP simulated without aerosol for PAR calculation and without aerosol for NIR calculation
E2	GPP simulated with aerosol for PAR calculation and without aerosol for NIR calculation
E3	GPP simulated without aerosol for PAR calculation and with aerosol for NIR calculation
E4	GPP simulated with aerosol for PAR calculation and with aerosol for NIR calculation

152

153 **3. BESS simulation and FLUXNET GPP comparison**

154 Firstly, we evaluate the accuracy of GPP simulated by BESS model. Due to the
155 comprehensive validation studies of BESS simulation [*Jiang and Ryu*, 2016; *Ryu et*
156 *al.*, 2011], here we only validate the general performance of BESS simulation in
157 China. Figure 1 shows the scatter plots of FLUXNET GPP observations against BESS
158 GPP simulations. The black line is the one-to-one line. These scatters are distributed
159 around the line. The sample size is about 1550 with R^2 of 0.552. Most of GPP values
160 range from 0 to 1. This is might due to the low GPP in GRA FLUXNET sites. The
161 RMSE is about 1.686. The GPP simulations from BESS are a little larger than
162 FLUXNET GPP observations.

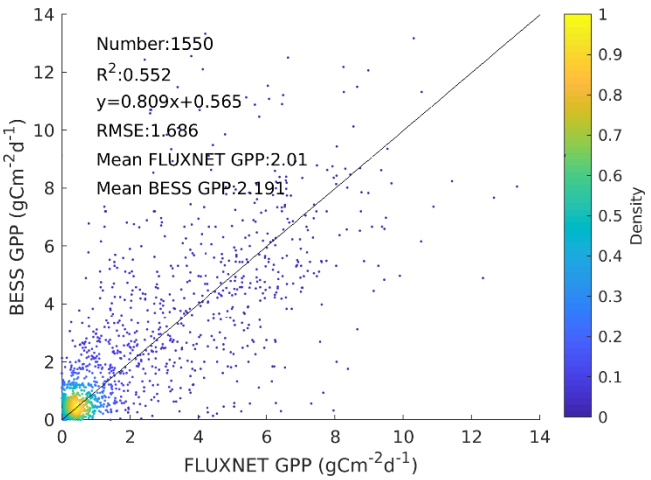

Figure 1. Scatter plots of BESS GPP simulations and FLUXNET measurements (black line represents the 1:1 line).

4. Sensitivity of GPP to AOD at FLUXNET sites

In order to evaluate the sensitivity of GPP to AOD, AOD from 0 to 3 at an interval of 0.1 was set for all days during 2002 to 2015. The PAR and NIR was calculated using SBDART with different AOD bins. Then, the GPP can be obtained through BESS model with a series of PAR and NIR. For each AOD bin, we did four experiments (Table 2). Figure 2 shows the variations of GPP with the increasing AOD. Yellow line means that only aerosol radiative effects in NIR was considered (E3-E1). Red line shows that only aerosol radiative effects in PAR was calculated for accessing the aerosol effects on GPP (E2-E1). Blue line represents that aerosol radiative effects in both NIR and PAR were included (E4-E1). The aerosol effects in NIR have little impacts on GPP over grassland and the GPP decreases with the increasing AOD in this kind of surface type. For forest sites, the aerosol effects in NIR is able to enhance the GPP and the fertilization of the aerosol effects in NIR increases with the aerosol loadings. Fertilization of aerosol effects in PAR can be found when the AOD is lower than 0.4/0.6 for two forest FLUXNET station. If the AOD>0.4/0.6, the fertilization of aerosol effects in PAR will decrease with AOD. Considering the aerosol effects in both PAR and NIR, the maximum GPP can be found when the AOD is 0.5 for CN-Din and 0.7 for CN-Qia. The aerosol could hinder the growth of forest when AOD is

greater than 1.4 for CN-Din and 2.1 for CN-Qia.

To evaluate the effects of cloud on the interaction of aerosol and plants, we also examine the sensitivity of GPP to AOD over cloudless conditions. In this situation, we assumed that there is no cloud during the whole study period. Figure 3 illustrates the sensitivity of GPP to AOD under cloudless condition. Compared with cloudy conditions, higher GPP is shown for all FLUXNET stations. For mixed forest site, the GPP increases with the aerosol loadings when the AOD is lower than 0.4 and then the GPP decreases with the AOD. This trend cannot be simulated in all-sky conditions. For grass stations, little differences of GPP decreasing trends between all-sky and cloudless conditions are found. However, the variations of GPP are larger under cloudless conditions than that under all-sky conditions. When we only consider the aerosol effects in PAR, the maximum GPP can be found when AOD is 0.8 for CN-Din and 1 for CN-Qia. The fertilization effects of aerosols in NIR are shown in both clear days and hazy days. The GPP rises from ~3.6 to ~3.9 $gCm^{-2}d^{-1}$ for CN-Din and from ~3.9 to ~4.2 $gCm^{-2}d^{-1}$ for CN- Qia. Considering aerosol effects in both PAR and NIR, maximum GPP can be found when AOD is 1 and 1.2 for EBF and ENF site. When the AOD is higher than 1-1.2, the GPP start falling. However, the fertilization effects still exist when the AOD reach to 3.

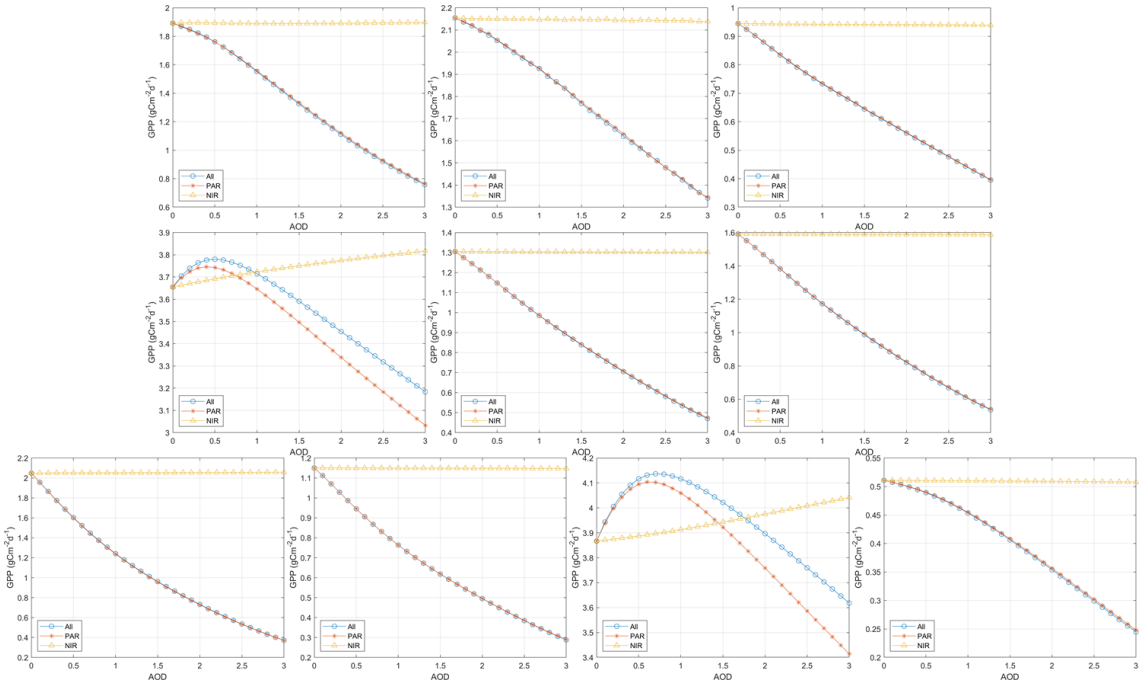

Figure 2. The sensitivity of GPP to AOD at ten FLUXNET sites (yellow line, red line, and blue line represent the effects of NIR, PAR, and all bands).

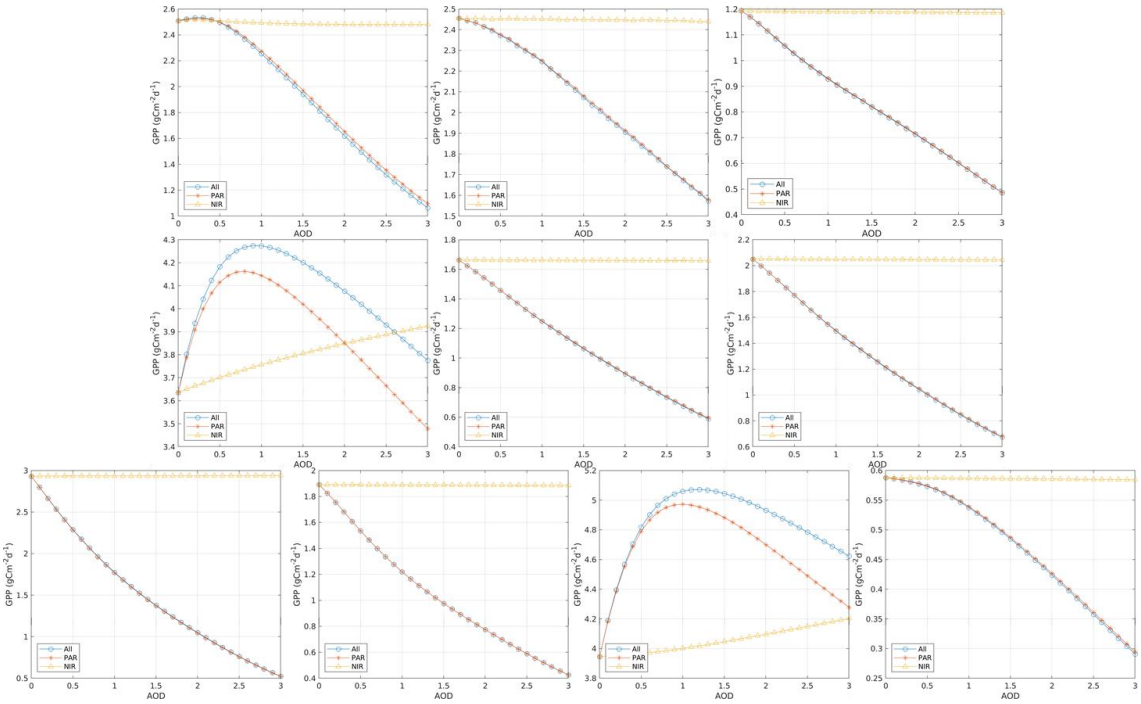

Figure 3. Same as Figure 2, but for cloudless condition.

5. The effects of aerosol pollution on GPP

To evaluate the radiative effects of current aerosol pollution on GPP, we used the MAIAC AOD, which is the most accurate aerosol products. Table 3 shows the effect of current aerosol loadings on GPP at FLUXNET sites in China. The result indicates that the effects of aerosol in PAR band reduce the growth of grass and mixed forests and enhance the growth of both EBF and ENF. The effects of aerosols on GPP in NIR is positive in EBF and ENF. Little impacts of aerosols on GPP in NIR are shown in MF, GRA, and WET FLUXNET sites. For effects of PAR, largest variation is shown in CN-Qia. For effects of NIR, most significant variation is shown in CN-Din. In all, the effects of current aerosol loadings on GPP is negative in MF, GRA, and WET, and positive in EBF and ENF.

Table 3. The multi-year effects of current aerosol pollutions on GPP at ten FLUXNET sites.

Station name	PAR	NIR	PAR and NIR

CN-Cha	-0.0915	0.0019	-0.0891
CN-Cng	-0.0788	-0.0020	-0.0788
CN-Dan	-0.0073	-0.0001	-0.0074
CN-Din	0.0643	**0.0397**	0.1042
CN-Du2	-0.0800	0.0006	-0.0790
CN-Du3	-0.0990	-0.0003	-0.0993
CN-Ha2	-0.1428	0.0016	-0.1412
CN-HaM	-0.0580	-0.0001	-0.0581
CN-Qia	**0.1688**	0.0186	**0.1867**
CN-Sw2	-0.0112	-0.0001	-0.0113

Table 4. The seasonal effects of current aerosol pollution on GPP at ten FLUXNET sites.

6. Discussion and conclusions

In this paper, we used the MODIS Atmosphere and Land products combined with the process-based model to test the sensitivity of GPP on AOD in all-sky and cloudless conditions and accurately evaluate the current aerosol loadings on terrestrial carbon fluxes in China. We found that the aerosol radiative effects on GPP not only varied with vegetation type but also varied with the spectral regions. The difference of aerosol effects in vegetation types are widely acknowledged [*Ezhova et al.*, 2018; *Niyogi et al.*, 2004]. However, the aerosol radiative effects on GPP in different spectral regions were seldom reported in our knowledge. The differences in spectral regions are because they have different features in atmospheric and canopy radiative transfer. In atmosphere, the magnitude of NIR influenced by aerosols is smaller than that of PAR [*Hatzianastassiou et al.*, 2007]. In addition, the photons are scattered more in the NIR region than PAR within the canopy [*Ryu et al.*, 2011]. These are the two mainly reasons for the difference of aerosol effects on GPP in PAR and NIR.

The estimation in this paper is highly dependent on the capacity of the BESS

model. Therefore, we assessed the performance of BESS GPP simulations against FLUXNET observations in China. The GPP simulated by FLUXNET can agree with the ground-based measurements well (R^2>0.55). The satellite AOD is also one of the uncertainties for simulating the radiative effects of aerosols. Previous study has demonstrated that the MAIAC aerosol products are highly consistent with the ground-based measurements in China (R>0.92) [*Zhang et al.*, 2019a]. The accuracy of MAIAC AOD is higher than model simulations [*Sun et al.*, 2019]. Therefore, we consider our results have high accuracy in simulating the aerosol radiative effects. Here, we only considered the aerosol radiative effects and ignored the environment effects of aerosols, such as temperature, vapor pressure deficit (VPD) and precipitation. *Huang et al.* [2006] examined the impacts of aerosols on surface temperature and found that the diurnal temperature range decreases by -0.7^{o}C over the industrialized regions in China. *Lee et al.* [2014] estimated that the precipitation reduction is about 40% due to the effects of absorbing aerosols. However, these papers also showed that the confidence of the result is limited by the uncertainties in modelling cloud physics. In addition, the ground-based measurements of aerosol-precipitation and aerosol-temperature interactions are still very limited and hardly to find a consistent conclusion. Therefore, only aerosol radiative effects were considered.

Although there are still some uncertainties, we firstly showed that aerosol radiative effects on GPP varied with vegetation type and spectral band. For NIR (700-4000 nm), little impacts of aerosols were shown over grass and wet land, while the forest GPP monotonously increased with the aerosol loadings when the AOD is lower than 3. For PAR (300-700), The GPP in grass land decreased with the AOD and the forest GPP firstly increases with the AOD and then decreased. The clouds play an important role in the aerosols-plants interaction and they restrain the effects of aerosols on growth of plants. The conclusion in this study can be used for fully understanding the effects of aerosol on land carbon uptake.

Acknowledgements

The authors would like to thank the team of BESS model (http://environment.snu.ac.kr/bess_flux/) for their hard work. We appreciate a large work of MODAPS team on MAIAC integration. We would like to thank the team of MODIS (https://ladsweb.modaps.eosdis.nasa.gov/search/) and FLUXNET (https://fluxnet.fluxdata.org/data/fluxnet2015-dataset/) for their great work. This study was supported by the Zhejiang Provincial Natural Science Foundation of China (Grant No. LQ18D010004), National Science Foundation of China (Grant No. 41801258).

References:

Ceamanos, X., D. Carrer, and J. L. Roujean (2014), Improved retrieval of direct and diffuse downwelling surface shortwave flux in cloudless atmosphere using dynamic estimates of aerosol content and type: application to the LSA-SAF project, *Atmospheric Chemistry and Physics*, *14*(15), 8209-8232.

Chameides, W. L., et al. (1999), Case study of the effects of atmospheric aerosols and regional haze on agriculture: An opportunity to enhance crop yields in China through emission controls?, *Proceedings of the National Academy of Sciences*, *96*(24), 13626.

Che, H., et al. (2019), Large contribution of meteorological factors to inter-decadal changes in regional aerosol optical depth, *Atmos. Chem. Phys.*, *19*(16), 10497-10523.

Chou, M.-D., P.-H. Lin, P.-L. Ma, and H.-J. Lin (2006), Effects of aerosols on the surface solar radiation in a tropical urban area, *Journal of Geophysical Research: Atmospheres*, *111*(D15), D15207.

Cirino, G. G., R. A. F. Souza, D. K. Adams, and P. Artaxo (2014), The effect of atmospheric aerosol particles and clouds on net ecosystem exchange in the Amazon, *Atmos. Chem. Phys.*, *14*(13), 6523-6543.

Cohan, D. S., J. Xu, R. Greenwald, M. H. Bergin, and W. L. Chameides (2002), Impact of atmospheric aerosol light scattering and absorption on terrestrial net primary productivity, *Global Biogeochemical Cycles*, *16*(4), 37-31-37-12.

Eck, T. F., J. Huttunen, K. E. J. Lehtinen, A. V. Lindfors, G. Myhre, A. Smirnov, S. N. Tripathi, and H. Yu (2013), Influence of observed diurnal cycles of aerosol optical depth on aerosol direct radiative effect,

295 *Atmospheric Chemistry and Physics*, *13*(15), 7895-7901.
296 Ezhova, E., et al. (2018), Direct effect of aerosols on solar radiation and gross primary production in
297 boreal and hemiboreal forests, *Atmos. Chem. Phys.*, *18*(24), 17863-17881.
298 Field, C. B., V. R. Barros, K. Mach, and M. Mastrandrea (2014), Climate change 2014: impacts,
299 adaptation, and vulnerability, *Working Group II Contribution to the IPCC 5th Assessment*
300 *Report-Technical Summary*, 1-76.
301 Frouin, R., and H. Murakami (2007), Estimating photosynthetically available radiation at the ocean
302 surface from ADEOS-II global imager data, *Journal of Oceanography*, *63*(3), 493-503.
303 Hatzianastassiou, N., C. Matsoukas, A. Fotiadi, J. P. W. Stackhouse, P. Koepke, K. G. Pavlakis, and I.
304 Vardavas (2007), Modelling the direct effect of aerosols in the solar near-infrared on a planetary scale,
305 *Atmos. Chem. Phys.*, *7*(12), 3211-3229.
306 Hinds, W. C. (1999), Aerosol Technology: Properties, *Behavior, and Measurement of airborne Particles*
307 *(2nd)*.
308 Huang, Y., R. E. Dickinson, and W. L. Chameides (2006), Impact of aerosol indirect effect on surface
309 temperature over East Asia, *Proceedings of the National Academy of Sciences of the United States of*
310 *America*, *103*(12), 4371.
311 Jiang, C., and Y. Ryu (2016), Multi-scale evaluation of global gross primary productivity and
312 evapotranspiration products derived from Breathing Earth System Simulator (BESS), *Remote Sensing of*
313 *Environment*, *186*, 528-547.
314 Lee, D., Y. C. Sud, L. Oreopoulos, K. M. Kim, W. K. Lau, and I. S. Kang (2014), Modeling the influences of
315 aerosols on pre-monsoon circulation and rainfall over Southeast Asia, *Atmospheric Chemistry and*
316 *Physics*, *14*(13), 6853-6866.
317 Liu, Y., J. R. Sun, and B. Yang (2009), The effects of black carbon and sulphate aerosols in China regions
318 on East Asia monsoons, *Tellus Series B-Chemical and Physical Meteorology*, *61*(4), 642-656.
319 Martins, V. S., A. Lyapustin, L. A. S. de Carvalho, C. C. F. Barbosa, and E. M. L. M. Novo (2017),
320 Validation of high-resolution MAIAC aerosol product over South America, *J Geophys Res-Atmos*,
321 *122*(14), 7537-7559.
322 Mercado, L. M., N. Bellouin, S. Sitch, O. Boucher, C. Huntingford, M. Wild, and P. M. Cox (2009), Impact
323 of changes in diffuse radiation on the global land carbon sink, *Nature*, *458*(7241), 1014-1017.
324 Misson, L., M. Lunden, M. McKay, and A. H. Goldstein (2005), Atmospheric aerosol light scattering and

surface wetness influence the diurnal pattern of net ecosystem exchange in a semi-arid ponderosa pine plantation, *Agricultural and Forest Meteorology*, *129*(1), 69-83.

Nagorski, S. A., S. D. Kaspari, E. Hood, J. B. Fellman, and S. M. Skiles (2019), Radiative Forcing by Dust and Black Carbon on the Juneau Icefield, Alaska, *Journal of Geophysical Research: Atmospheres*, *0*(ja).

Niyogi, D., et al. (2004), Direct observations of the effects of aerosol loading on net ecosystem CO2 exchanges over different landscapes, *Geophysical Research Letters*, *31*(20).

O'Sullivan, M., A. Rap, C. L. Reddington, D. V. Spracklen, M. Gloor, and W. Buermann (2016), Small global effect on terrestrial net primary production due to increased fossil fuel aerosol emissions from East Asia since the turn of the century, *Geophysical Research Letters*, *43*(15), 8060-8067.

Qian, Y., W. G. Wang, L. R. Leung, and D. P. Kaiser (2007), Variability of solar radiation under cloud-free skies in China: The role of aerosols, *Geophysical Research Letters*, *34*(12), L12804.

Rap, A., et al. (2018), Enhanced global primary production by biogenic aerosol via diffuse radiation fertilization, *Nature Geoscience*, *11*(9), 640-644.

Ricchiazzi, P., S. Yang, C. Gautier, and D. Sowle (1998), SBDART: A Research and Teaching Software Tool for Plane-Parallel Radiative Transfer in the Earth's Atmosphere, *B Am Meteorol Soc*, *79*(10), 2101-2114.

Ryu, Y., C. Jiang, H. Kobayashi, and M. Detto (2018), MODIS-derived global land products of shortwave radiation and diffuse and total photosynthetically active radiation at 5km resolution from 2000, *Remote Sensing of Environment*, *204*, 812-825.

Ryu, Y., et al. (2011), Integration of MODIS land and atmosphere products with a coupled-process model to estimate gross primary productivity and evapotranspiration from 1 km to global scales, *Global Biogeochemical Cycles*, *25*(4).

Strada, S., N. Unger, and X. Yue (2015), Observed aerosol-induced radiative effect on plant productivity in the eastern United States, *Atmospheric Environment*, *122*, 463-476.

Sun, E., X. Xu, H. Che, Z. Tang, K. Gui, L. An, C. Lu, and G. Shi (2019), Variation in MERRA-2 aerosol optical depth and absorption aerosol optical depth over China from 1980 to 2017, *Journal of Atmospheric and Solar-Terrestrial Physics*, *186*, 8-19.

Tang, J., P. Wang, L. J. Mickley, X. Xia, H. Liao, X. Yue, L. Sun, and J. Xia (2014), Positive relationship between liquid cloud droplet effective radius and aerosol optical depth over Eastern China from satellite data, *Atmospheric Environment*, *84*(0), 244-253.

Tie, X., R. J. Huang, W. Dai, J. Cao, X. Long, X. Su, S. Zhao, Q. Wang, and G. Li (2016), Effect of heavy

haze and aerosol pollution on rice and wheat productions in China, *Sci Rep*, *6*, 29612.

Tie, X. X., and J. J. Cao (2009), Aerosol pollution in China: Present and future impact on environment, *Particuology*, *7*(6), 426-431.

Wong, M. S., J. Nichol, K. H. Lee, and Z. Li (2008), Retrieval of aerosol optical thickness using MODIS 500× 500m 2, a study in Hong Kong and Pearl River Delta region, paper presented at Earth Observation and Remote Sensing Applications, 2008. EORSA 2008. International Workshop on, IEEE.

Wu, S., et al. (2014), Association of cardiopulmonary health effects with source-appointed ambient fine particulate in Beijing, China: a combined analysis from the Healthy Volunteer Natural Relocation (HVNR) study, *Environmental science & technology*, *48*(6), 3438-3448.

Yamaguchi, M., and T. Izuta (2017), Effects of Aerosol Particles on Plants, in *Air Pollution Impacts on Plants in East Asia*, edited by T. Izuta, pp. 283-293, Springer Japan, Tokyo.

Yu, H. (2004), Direct radiative effect of aerosols as determined from a combination of MODIS retrievals and GOCART simulations, *Journal of Geophysical Research*, *109*(D3).

Yue, X., and N. Unger (2017), Aerosol optical depth thresholds as a tool to assess diffuse radiation fertilization of the land carbon uptake in China, *Atmos. Chem. Phys.*, *17*(2), 1329-1342.

Yue, X., and N. Unger (2018), Fire air pollution reduces global terrestrial productivity, *Nature Communications*, *9*(1), 5413.

Zamora, L. M., R. A. Kahn, S. Eckhardt, A. McComiskey, P. Sawamura, R. Moore, and A. Stohl (2017), Aerosol indirect effects on the nighttime Arctic Ocean surface from thin, predominantly liquid clouds, *Atmos. Chem. Phys.*, *17*(12), 7311-7332.

Zhang, Z. Y., M. S. Wong, and K. H. Lee (2015), Estimation of potential source regions of PM2.5 in Beijing using backward trajectories, *Atmospheric Pollution Research*, *6*(1), 173-177.

Zhang, Z. Y., W. L. Wu, M. Fan, J. Wei, Y. H. Tan, and Q. Wang (2019a), Evaluation of MAIAC aerosol retrievals over China, *Atmospheric Environment*, *202*, 8-16.

Zhang, Z. Y., W. L. Wu, M. Fan, M. H. Tao, J. Wei, J. Jin, Y. H. Tan, and Q. Wang (2019b), Validation of Himawari-8 aerosol optical depth retrievals over China, *Atmospheric Environment*, *199*, 32-44.